Cancer Science
Japanese Cancer Association JCA
Open Access

# Notch4+ cancer stem-like cells promote the metastatic and invasive ability of melanoma

Xian Lin,[1,6] Baocun Sun,[1,2,3,6] Dongwang Zhu,[4] Xiulan Zhao,[1,3] Ran Sun,[5] Yanhui Zhang,[2] Danfang Zhang,[1] Xueyi Dong,[1] Qiang Gu,[1,3] Yanlei Li[1] and Fang Liu[1]

[1]Department of Pathology, Tianjin Medical University, Tianjin; [2]Department of Pathology, Cancer Hospital of Tianjin Medical University, Tianjin; [3]Department of Pathology, General Hospital of Tianjin Medical University, Tianjin; [4]Department of Surgery, Stomatological Hospital of Tianjin Medical University, Tianjin; [5]Department of Surgery, Tianjin Hospital of ITCWM Nankai Hospital, Tianjin, China

**Key words**

Cancer stem cell, epithelial–mesenchymal transition, melanoma, Notch4 protein, Twist1

**Correspondence**

Baocun Sun, Department of Pathology and Cancer Hospital and General Hospital of Tianjin Medical University, Tianjin 300070, China.
Tel: +86-136-0211-1192; Fax: 86-22-8333-6813;
E-mail: baocunsun@aliyun.com

[6]These authors contributed equally to this work.

**Funding Information**

National Natural Science Foundation of China (81230050, 81572872).

Received March 14, 2016; Revised May 17, 2016; Accepted May 26, 2016

*Cancer Sci* **107** (2016) 1079–1091

doi: 10.1111/cas.12978

**Sphere formation in conditioned serum-free culture medium supplemented with epidermal growth factor and basic fibroblast growth factor (tumorospheres) is considered useful for the enrichment of cancer stem-like cells, also known as tumor-initiating cells. We used a gene expression microarray to investigate the gene expression profile of melanoma cancer stem-like cells (MCSLCs). The results showed that MCSLCs highly expressed the following Notch signaling pathway molecules: Notch3 (NM_008716), Notch4 (NM_010929), Dtx4 (NM_172442), and JAG2 (NM_010588). Immunofluorescence staining showed tumorosphere cells highly expressed Notch4. Notch4$^{high}$ B16F10 cells were isolated by FACS, and Western blotting showed that high Notch4 expression is related to the expression of epithelial–mesenchymal transition (EMT)-associated proteins. Reduced invasive and migratory properties concomitant with the downregulation of the EMT markers Twist1, vimentin, and VE-cadherin and the overexpression of E-cadherin was observed in human melanoma A375 and MUM-2B cells. In these cells, Notch4 was also downregulated, both by *Notch4* gene knockdown and by application of the γ-secretase inhibitor, DAPT. Mechanistically, the re-overexpression of Twist1 by the transfection of cells with a Twist1 expression plasmid led to an increase in VE-cadherin expression and a decrease in E-cadherin expression. Immunohistochemical analysis of 120 human melanoma tissues revealed a significant correlation between the high expression of Notch4 and the metastasis of melanoma. Taken together, our findings indicate that Notch4+ MCSLCs trigger EMT and promote the metastasis of melanoma cells.**

Accumulating evidence has revealed that malignant solid tumors, including melanoma, contain cancer stem-like cells, also known as tumor-initiating cells.[1–5] The properties of infinite proliferation, self-renewal, and chemoresistance as well as the ability of these cells to differentiate into mature, specialized cancer cell types may be responsible for tumor initiation, metastasis, and the high mortality rate of cancer patients.[6–8] Recent research identified a side-population of cells and several proteins as markers for cancer stem cells (CSCs).[9,10] CD44, CD133, ABCG2, ABCB5, OCT4, and CD271 (nerve growth factor receptor [NGFR]) are considered markers of melanoma CSCs.[11–14] Alternatively, as a functional approach, the enrichment of a potential CSC subpopulation may be accomplished using a sphere formation assay. In this assay, conditioned serum-free culture medium (SFM) supplemented with epidermal growth factor and basic fibroblast growth factor is used in the generation of tumorospheres; this method has been considered useful for the enrichment of CSCs.[12,15–17] Recent studies have revealed the plasticity of cancer cells, as differentiated cancer cells can transform through epithelial–mesenchymal transition (EMT) so that they possess cancer stem-like properties.[18] Other researchers revealed that sphere-forming cells have enhanced migratory/invasive properties.[6,19–21]

To further investigate melanoma cancer stem-like cells (MCSLCs), we analyzed MCSLCs that were enriched by the tumorosphere formation assay described above. We also used a gene expression microarray to investigate the gene expression profile of MCSLC. Our results indicated that the Notch4 protein was significantly highly expressed in MCSLCs, which indicates a poor prognosis in individuals with melanoma. Moreover, Notch4 promotes metastasis of melanoma through the Twist/VE-cadherin/E-cadherin pathway.

## Materials and Methods

**Melanoma cell lines, tumorospheres, and multicellular tumor spheroid model.** The B16F10, A375 A875, MUM-2C and MUM-2B melanoma cell lines were obtained from China Infrastructure of Cell Line Resources (Beijing, China).

Tumorospheres and the multicellular tumor spheroid (MTS) model were cultured in a serum-free system as previously described.[22,23] Third-generation/tertiary suspension cells were used for all subsequent experiments.

**Microarray and bioinformatic analyses.** The total RNA of tumorospheres (test group) and MTS (control group) were extracted using TRIzol reagent (Invitrogen, Carlsbad, CA, USA). Briefly, the extracted RNA was labeled and hybridized on an Agilent Mouse Gene Expression Microarray (8*60K, design ID: 028005; Agilent Technologies, Santa Clara, CA, USA) by Oebiotech Co. (Shanghai, China). Statistical analyses and data normalization were carried out using GeneSpring (version 12.5) software (Agilent Technologies). Differentially expressed genes were then identified through fold changes as well as through *P*-values calculated by *t*-test. The threshold set for upregulated and downregulated genes was a fold change $\geq$2.0 and a *P*-value $\leq$0.05.

**Fluorescence-activated cell sorting.** B16F10 cells cultured as a monolayer were digested with EDTA–trypsin and collected. Non-specific antigens were blocked with 0.5% FBS. A Notch4 antibody (Abcam, Cambridge, MA, USA) was added to the B16F10 cells at a 1:400 dilution. The cells were then incubated for 1 h with an Alexa Fluor 488 goat anti-rabbit IgG, which served as the secondary antibody, at a 1:1000 dilution. Labeled B16F10 cells were sorted by a FACS Vantage SE/DiVa cell sorter with FACS DiVa software (BD Biosciences, San Jose, CA, USA).

**Cell immunofluorescence method.** The cells were plated onto coverslips and fixed with cold methanol on ice for 10 min. The cells were blocked with 5% FCS and were incubated with primary antibodies Notch4 (1:500 dilution) and vimentin (1:250 dilution) overnight at 4°C. Then FITC-conjugated secondary antibodies were added and the cells were incubated at 37°C for 1 h. The sections were counterstained with DAPI and were observed using a fluorescence microscope at $\times$200 magnification (80i; Nikon, Shinagawa, Tokyo, Japan).

**Western blot analysis.** The cell lysates were resolved by SDS-PAGE and transferred onto PVDF membranes (Millipore, Billerica, MA, USA). Blots were blocked and incubated with primary antibodies overnight at 4°C. The membranes were then incubated with the secondary antibody at 37°C for 2 h. The enhanced chemiluminescence method was used to measure protein expression, and GAPDH served as the internal control. Bands were imaged and analyzed using C-Digit Blotting Scanner (Gene Company, Beijing, China). Details of the antibodies used are shown in Table S1.

**Matrigel-based tube formation assay.** The Matrigel-based tube formation assay was carried out as previously described.[24] Matrigel (BD Biosciences) was warmed to room temperature. Before completely thawed, it was transferred onto ice where the liquid was kept for at least 10 min. Then 30 μL Matrigel was added to 96-well plates at a horizontal level so that the Matrigel was allowed to distribute evenly. The coated plates were incubated for 1 h at 37°C. After the cells ($2 \times 10^4$) were loaded onto the Matrigel, they were allowed to incubate overnight. The cells were then imaged at $\times$40 magnification.

**Hoechst 33342 staining.** A375 and MUM-2B cells were transfected with the LVRU6MP vector, which expressed mCherry fluorescent protein. Hoechst 33342 dye was added at a final concentration of 5 μg/mL, then the cells were incubated at 37°C for 30 min. After incubation, the cells were gently washed twice in PBS prior to microscopy and image capture.

***Notch4* gene silencing.** To further detect the role of Notch4 in melanoma cells, stable *Notch4* silenced cell lines were generated. Notch4 suppression was mediated by lentiviral infection using OmicsLink shRNA expression clones (catalog no. HSH011877-LVRU6MP; GeneCopoeia, Rockville, MD, USA). The target sequence is described in Table S2 and is shown in figures from "shNotch4-1"to "shNotch4-4". A non-silencing shRNA sequence without the Notch4 shRNA component was used as the negative control (catalog no.: CSHCTR001-LVRU6MP). Approximately $3 \times 10^5$ melanoma cells/well were plated in 6-well plates. Twenty-four hours later, A375 and MUM-2B cells were transfected with specific or negative control lentiviral vectors with the Lenti-Pac HIV packaging kit (catalog no. HPK-LvTR-20; Genecopoeia) according to the manufacturer's instructions. Ninety-six hours after transfection, the transfected cells were observed under a fluorescence microscope (Nikon). As the lentiviral vector contains an mCherry Fluorescent Protein (mCFP) expression cassette, the cell transfection rate, which was directly observable, reached 90%.

**Transwell invasion/migration assay.** In all, $1 \times 10^5$ cells in 100 μL culture medium without FBS were seeded into the upper chamber with or without Matrigel (1 mg/mL; BD Biosciences); the wells contained polyethylene terephthalate filters with a porosity of 8 mm (Invitrogen). The lower chamber was filled with medium supplemented with 10% FBS. After 36 h for MUM-2B cells and 48 h for A375 cells, the invading or migrating cells were fixed in cold methanol and stained with 0.5% crystal violet. The number of invading/migrating cells was counted in three fields using an inverted light microscope (Nikon) at $\times$100 magnification. Each experiment was carried out in triplicate.

**Wound healing assay.** In all, $5 \times 10^5$ cells were seeded and allowed to grow to 90% confluence. A wound was created on the cell monolayer using a pipette tip, and cell motility was assessed by measuring the amount of cell movement into the scraped area. Images were captured at regular time intervals. The speed of wound closure was monitored after 12 and 24 h by a measurement of the ratio of the distance of the wound at 0 h. Each experiment was carried out in triplicate.

**Real-time PCR.** Total RNA from melanoma cells was isolated using TRIzol reagent (Invitrogen). Synthesis of cDNA was carried out with a QuantScript RT Kit (Tiangen Biotech, Beijing, China) according to the manufacturer's instructions. Quantitative RT-PCR was carried out in an ABI 7500 Real-Time PCR System (Applied Biosystems, Foster City, CA, USA) with real-time PCR Master Mix (SYBR Green). The PCR primers are listed in Table S2. GAPDH was selected as the endogenous control in this assay, and the $2^{-\Delta\Delta Ct}$ method was used to analyze the relative gene expression data.[25]

**Drug treatment.** For the suppression of Notch signaling, DAPT was prepared as a 10-μM stock in DMSO (catalog no. D5942; Sigma-Aldrich, St. Louis, MO, USA). Cells were treated with DMSO or DAPT (10 μM) and were analyzed after 72 h.

**Collection of patient samples.** In all, 120 primary tumor specimens were obtained from the Tumor Tissue Bank of the Tianjin Cancer Hospital (Tianjin, China). The specimens were excised from patients with melanoma who underwent surgical resection at the Tianjin Medical University Cancer Institute and Hospital in China between January 1999 and December 2010.

All tissue sections were reviewed by a pathologist and were assessed according to the 2010 WHO Classification of Tumors: Pathology and Genetics of Skin Tumors. The use of patient specimens was approved by the Institutional Research Committee. Detailed pathologic and clinical data were collected for all samples and are shown in Table S3.

**Immunohistochemical staining and scoring.** Immunohistochemistry was carried out as previously described.[26] Tissue sections were deparaffinized and rehydrated and the endogenous peroxidase was quenched. After antigen retrieval using a microwave and the blocking of non-specific binding, the

sections were then incubated with anti-Notch4 antibody (catalog no. ab134831; Abcam) at a dilution of 1:500 overnight at 4°C. Phosphate-buffered saline was used as a negative control in place of the primary antibody. The sections were then incubated with the secondary antibody, developed with 3,3′-diaminobenzidine and counterstained with hematoxylin.

Evaluation of the sections was carried out independently by two pathologists, and the staining results were semiquantitatively assessed according to both the percentage of positive neoplastic cells and the immunostaining intensity in individual tumor cells. In all, 100 tumor cells per field in 10 microscopic fields in each section were counted at a high magnification. The initial scoring was undertaken based on the extent of staining on a scale of 0–4, as follows: 0, ≤10%; 1, 10–25%; 2, 26–50%; 3, 51–75%; and 4, ≥76–100%. The intensity of staining was scored on a scale of 0–3, as follows: 0, no appreciable staining in tumor cells; 1, barely detectable staining in the cytoplasm compared with the stromal elements; 2, moderate staining; 3, strong staining in tumor cells that obscures the cytoplasm. After the values were summed (extent + intensity), the scores ranged from 0 to 6. With regards to statistical analysis, a total score of 0–2 was considered low expression; scores of 3–6 were considered high expression.

**Statistical analysis.** All data were analyzed with SPSS 19.0 (SPSS, Chicago, IL, USA). The measurement data are shown as the mean ± SD. Student's *t*-test was used to determine the differences between two groups. The $\chi^2$-test was used to test the relationship of Notch4 expression and melanoma. The survival rates were calculated by the life table method and the Wilcoxon test for statistical analysis. $P < 0.05$ was considered statistically significant.

## Results

Gene expression in MCSLCs enriched by the tumorosphere formation assay**.** To investigate the gene expression profile of MCSLCs (by the tumorosphere formation assay), an Agilent Mouse Gene Expression Microarray was used. Cultured suspension cells that were used to generate an MTS model were used as controls.

The gene expression analysis showed 3760 differentially expressed genes, including 1699 upregulated genes and 2061 downregulated genes (Fig. 1a). The expression levels of Notch3 (NM_008716), Notch4 (NM_010929), Dtx4 (NM_172442), JAG2 (NM_010588) Pofut (NM_080463), Sox4 (NM_009238), Wnt10a (NM_009518), NGFR (NM_033217),

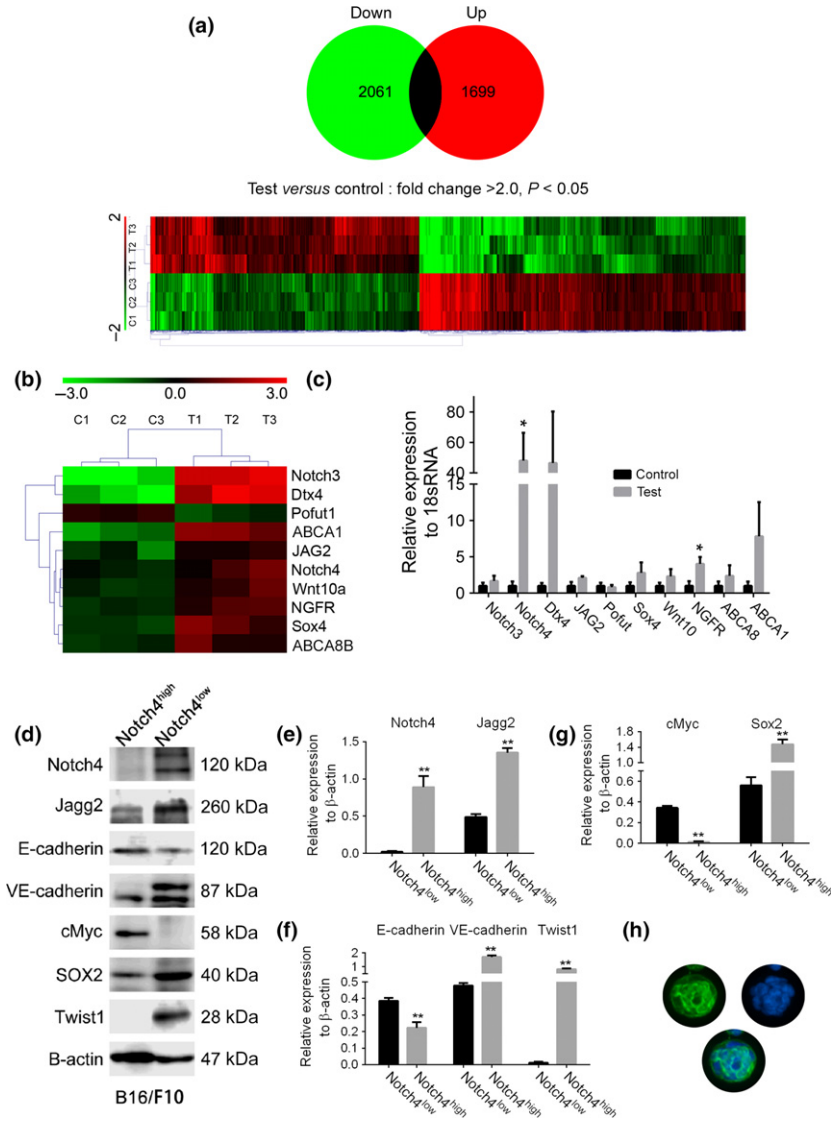


**Fig. 1.** Notch4 was highly expressed in melanoma cancer stem-like cells (MCSLCs) and was associated with the expression of epithelial–mesenchymal transition (EMT) proteins. (a) Agilent Mouse 8x60K microarrays were used to analyze gene expression in MCSLCs enriched from tumorospheres of B16F10 cells (test group) (multicellular tumor spheroid of B16F10 cells were used as a control). The gene expression analysis showed 3760 differentially expressed genes, including 1699 upregulated genes and 2061 downregulated genes (genes with a fold change ≥2 and a *P*-value (*t*-test) <0.05 were collected). (b) Changes in the expression of Notch3, Notch4, Dtx4, JAG2, Pofut, SOX4, Wnt10a, NGFR, ABCA8, and ABCA1. (c) Quantitative real-time PCR identified changes in expression levels. (d) Notch4$^{high}$ B16F10 cells were isolated and found to express high levels of Twist1 and VE-cadherin, whereas the expression of E-cadherin was inhibited. (e–g) Grey analysis showed that the differences were statistically significant. (h) Sphere-forming B16F10 cells (MCSLCs) expressed high levels of Notch4 protein. *$P < 0.05$, **$P < 0.001$.

ABCA8 (NM_013851), and ABCA1 (NM_013454) were assessed. The fold changes according to the gene expression arrays are shown in Figure 1(b). Moreover, quantitative real-time (q)RT-PCR was carried out to identify the changes in expression levels. The qRT-PCR results showed that MCSLCs expressed higher levels of the cancer stem cell-related gene *NGFR* (also called CD271).[27] The qRT-PCR results also showed that Notch4 was significantly highly expressed in MCSLCs (Fig. 1c). Then, we determined whether an association could be found between *Notch4* overexpression and stem cell properties, invasion, or metastasis in melanoma.

The morphological differences of these two kind of melanoma spheroids are shown in Figure S1.

Notch4$^{high}$ B16F10 cells expressed high levels of EMT-related proteins and MCSLCs expressed high levels of Notch4 protein. To detect the role of Notch4 expression in melanoma, Notch4$^{high}$ B16F10 cell was isolated by FACS. The efficiency of isolation and the subsequent determination of EMT-related protein expression were ascertained by Western blotting.

Flow cytometry results showed that 2.8% of B16F10 cells expressed Notch4 protein on the cell surface. Results of Western blot analysis are illustrated in Figure 1(d). A Grey analysis revealed that Notch4$^{high}$ B16F10 cells expressed high levels of Notch4 and Jagg2 proteins (Fig. 1e). The EMT-related index of VE-cadherin and Twist1 expression showed that these two proteins were expressed at higher levels in Notch4$^{high}$ B16F10 cells compared with Notch4$^{low}$ B16F10 cells (Fig. 1f). Notch4$^{high}$ B16F10 cells also showed higher Sox2 expression and lower cMyc expression (Fig. 1g). As immunofluorescence staining illustrated, sphere-forming B16F10 cells expressed high levels of Notch4 protein (Fig. 1h).

Notch4 expression in human melanoma cell lines and its relationship to sphere formation. We next detected the expression of Notch4 protein in the human melanoma cell lines A875, A375, MUM-2C, and MUM-2B. Western blotting results showed that A375 and MUM-2B cells expressed high levels of Notch4 protein (Fig. 2a). Immunofluorescence staining identified the expression of Notch4 in A375 and MUM-2B cells (Fig. 2b). As shown in Figure 2(c), sphere-forming of A375 and MUM-2B cells expressed high levels of Notch4 protein. Both A375 and MUM-2B cells that were transfected with the psi-LVRU6MP vector, which expressed the mCherry protein, demonstrated vasculogenic mimicry (VM) (Fig. 2c, red circle and white line delineates tumor cells that formed VM). Then we chose MUM-2B and A375 human melanoma cell lines to determine the role of Notch4 in melanoma.

***Notch4* silencing inhibited invasion, migration, and VM formation of melanoma cells.** *Invasion and migration assay.* To detect the role of Notch4 in the invasion and migration of melanoma cells, Transwell invasion and migration assay was used.

As shown in Figure 3(a), except for the shNotch4-2 plasmid, all three shNotch4 plasmids inhibited the migration of A375 cells. Moreover, the four shNotch4 plasmids significantly reduced the invasiveness of the melanoma cell line A375, and these differences were statistically significant (Fig. 3c; $*P < 0.05$, $**P < 0.001$, control group *vs* signal shNotch4

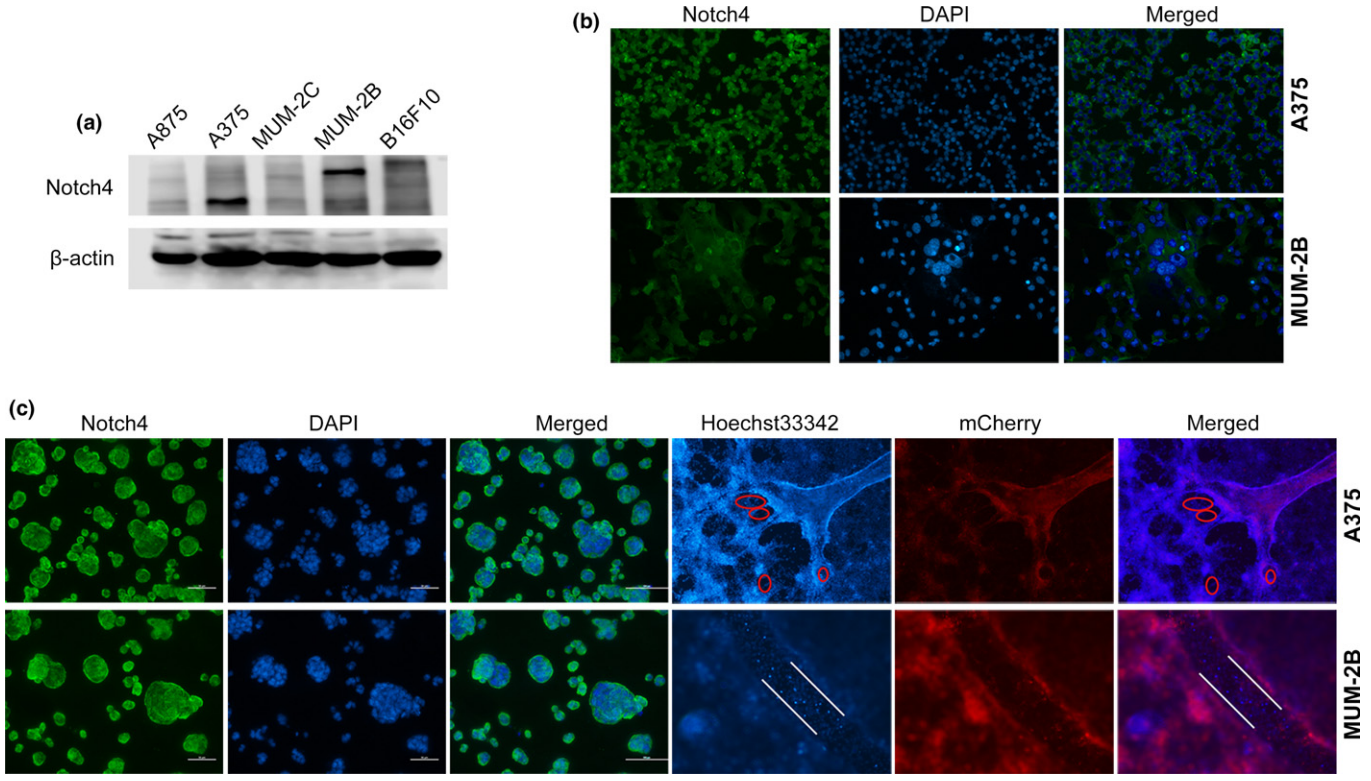


**Fig. 2.** A375 and MUM-2B cells expressed high levels of Notch4 and showed the capacity of vasculogenic mimicry (VM) formation. (a) Expression of Notch4 in melanoma cell lines A875, A375, MUM-2C, MUM-2B, and B16F10 was detected by Western blotting. A375 and MUM-2B cells expressed high levels of Notch4. The Notch4 protein is a ~210-kDa heterodimer. The Notch4 protein was split in the lysate, therefore, Western blot analysis detected both the intracellular and extracellular domains of Notch4. (b) Immunofluorescence staining confirmed high Notch4 expression in A375 and MUM-2B cells. (c) Sphere-forming A375 and MUM-2B cells expressed high levels of Notch4 protein. Hoechst 33342 staining and mCherry fluorescent protein expression showed that A375 and MUM-2B cells could form VM tubes *in vitro*. The red circle and white line delineate tumor cells that formed VM. A375 cells, ×40 magnification; MUM-2B cells, ×200 magnification.

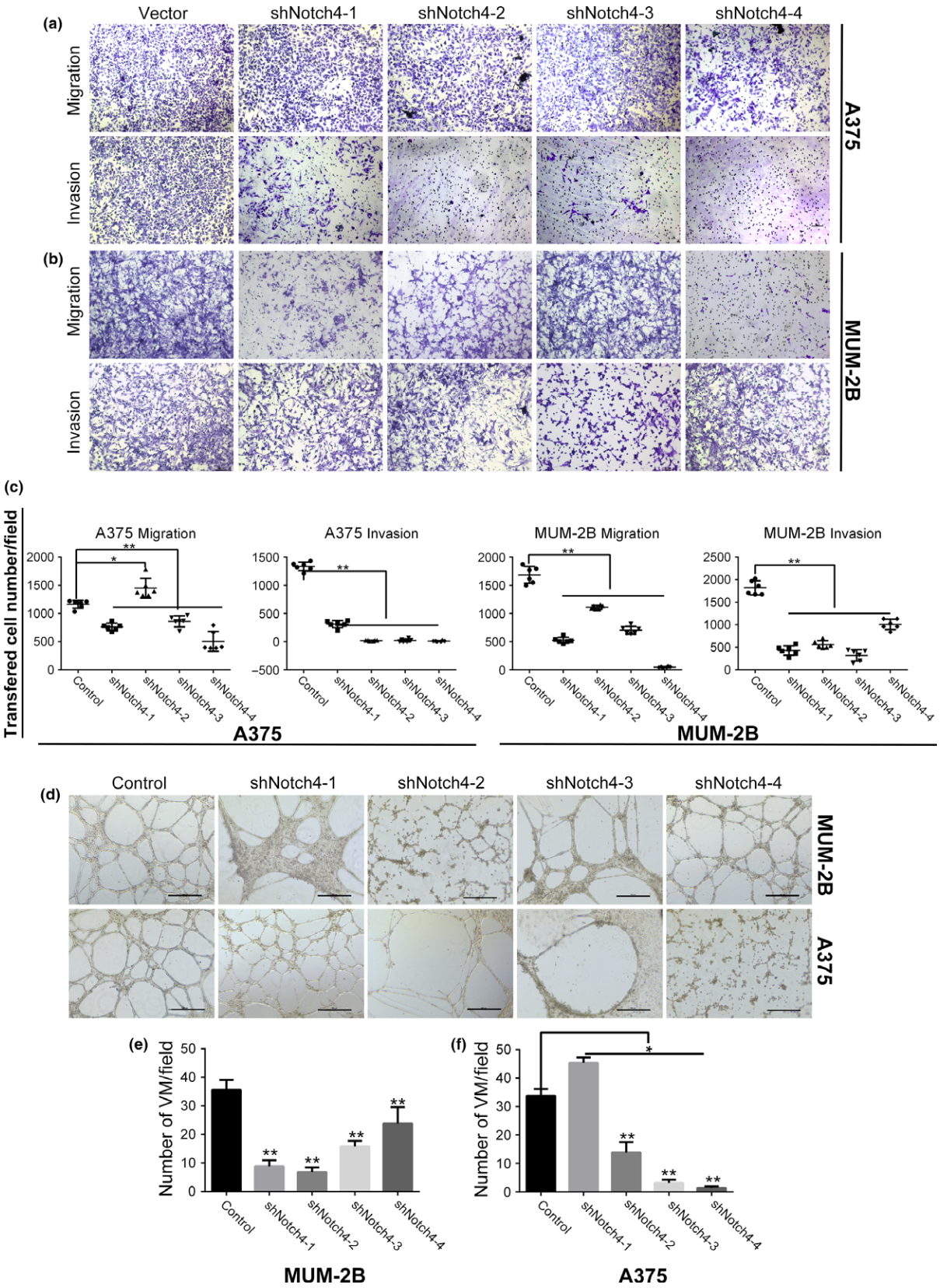


**Fig. 3.** *Notch4* silencing reduced cell invasion, migration, and vasculogenic mimicry (VM) formation in melanoma cells. (a–c) The invasion and migration abilities of A375 cells transfected with the LVRU6MP–shNotch4-1, -3, and -4 clones and of MUM-2B cells transfected with the LVRU6MP–shNotch4-1, -2, -3, and -4 clones were decreased following Notch4 knockdown. The differences have statistical significance. The shNotch4-2 plasmid increased the migration of A375 cells. $^{**}P < 0.001$. Magnification, ×100. (d–f) Capacity for VM formation of A375 cells transfected with the LVRU6MP–shNotch4-2, -3, and -4 plasmid and that of MUM-2B cells transfected with the LVRU6MP–shNotch4-1, -2, -3, and -4 plasmids was inhibited. The shNotch4-1 plasmid increased VM formation of A375 cells. $^{**}P < 0.001$. Magnification, ×40.

group). All four shNotch4 plasmids inhibited the migration and invasion abilities of MUM-2B cells (Fig. 3b,c; $*P < 0.05$, $**P < 0.001$, control group *vs* signal shNotch4 group). Our data suggest that Notch4 expression in melanoma cells is related to the invasiveness and migration ability of melanoma cells.

*Vasculogenic mimicry formation assay.* To detect the role of Notch4 in the formation of VM, a Matrigel-based tube formation assay was used (Fig. 3d). As Figure 3(e) shows, MUM-2B cells were transfected with four shNotch4 plasmids, which significantly reduced the number of VM *in vitro* ($**P < 0.001$). Although transfection with the shNotch4-1 plasmid increased the number of VM in A375 cells, transfection with the other three shNotch4 plasmids caused a statistically significant decrease in the number of VM (Fig. 3f) ($*P < 0.05$, $*P < 0.001$). We speculate that Notch4 expression is related to the VM formation of melanoma.

*Wound healing assay.* To detect the relationship between Notch4 expression and the migration of melanoma cells, a wound healing assay was undertaken (Fig. 4a). All four shNotch4 plasmids that were transfected to A375 and MUM-2B cells could inhibit the migration ability of these cells. The differences among the normal/control group, the A375 cells that were transfected with shNotch4 plasmids (at 24 h), and the MUM-2B cells that were transfected with the same plasmids (at 12 h) were statistically significant (Fig. 4b,c, $P < 0.05$). Therefore, we believe that Notch4 expression may be related to the migration of melanoma cells.

*Notch4* silencing decreased expression of EMT-related proteins in melanoma cells**.** Because Notch pathway suppression by shRNA inhibited the invasiveness, migration, and VM formation of melanoma cells, we analyzed several potential downstream targets that were previously shown by our group and others to be associated with EMT of tumor cells.[28–31] To determine the role of *Notch4* silencing with respect to the EMT-related index, immunofluorescence staining, Western blot assay, and quantitative real-time PCR were carried out.

Vimentin expression followed by Notch4 suppression in A375 and MUM-2B cells was validated by immunofluorescence staining (Fig. 4d). Results of Western blot analysis of A375 and MUM-2B cells are shown in Figures 5 and 6. The effects of transfection were then tested and analyzed (Figs 5b and 6b). Western blot results also showed that the expression of cMyc and Sox2 was increased in A375 cells, whereas the expression of these proteins was decreased in the MUM-2B cell line (Figs 5c and 6c).

Grey analysis showed that Notch4 suppression upregulated the expression of E-cadherin and downregulated the expression of VE-cadherin and Twist1 (Figs 5d and 6d). In the A375 cell lines, vascular endothelial growth factor (VEGF) expression was downregulated by the shNotch4-3 and shNotch4-4 plasmids, whereas VEGF was upregulated by the shNotch4-1 and shNotch4-2 plasmids (Fig. 5e). However, in the MUM-2B cell line, VEGF expression was reduced following the downregulation of Notch4 expression (Fig. 6e).

In conclusion, VEGF expression was positively regulated by Notch4 expression; thus, our data indicate that Notch4 expression is involved in EMT and tumor angiogenesis.

To further explore the role of Notch4 in EMT formation, we undertook the qRT-PCR assay (Figs 5f and 6f). The qRT-PCR results showed that Notch4 blocking downregulated VE-cadherin and Twist1 mRNA expression and gained E-cadherin mRNA expression. We deduced that Notch4 promoted cell invasion, migration, and VM formation by promoting EMT through the Twist1/VE-cadherin/E-cadherin pathway.

*Notch4* silencing reduced EMT through the Twist1/E-cadherin/VE-cadherin pathway**.** To block Notch signaling, we used DAPT, a γ-secretase inhibitor that is known to efficiently block Notch receptor cleavage in intact cells. Western blot analysis was used to detect Twist1 and E-cadherin expression. The results in Figure 7(a) show an increase in E-cadherin expression and loss of Twist1 and VE-cadherin expression in the DAPT treatment groups.

We then sought to determine whether Notch4 regulates VE-cadherin and E-cadherin through the control of Twist1 expression. To accomplish this, full-length Twist1 cDNA was subcloned into pcDNA3.1 vectors that were transfected into A375-shNotch4-3 and MUM-2B-shNotch4-3 cells.[31] Western blot results showed that E-cadherin expression was downregulated, whereas VE-cadherin expression in these cells was upregulated by Twsit1 re-overexpression. Our data therefore suggest that Notch4 promotes EMT through the regulation of Twist1 expression (Fig. 7b).

High expression of Notch4 was related to metastasis in patients with melanoma**.** To explore the role of Notch4 in the metastasis of melanoma, we collected 120 melanoma tissues from the Department of Pathology of the Cancer Hospital of Tianjin Medical University, and evaluated Notch4 protein expression by immunohistochemistry.

Seventy-two (72/120; 60%) melanoma tissues in our cohort expressed high levels of Notch4 protein. We retrospectively analyzed the clinicopathological parameters of these 120 cases of melanoma (Table 1). As Figure 7(c) and Table 1 show, high expression of Notch4 correlates with tumor metastasis, especially lymphatic metastasis.

High expression of Notch4 indicated poor prognosis**.** We next determined the relationship between Notch4 expression and the prognosis of patients with melanoma using the life table method (details are shown in Table S4). The 3- and 5-year survival rates and the median survival time (life table method) of melanoma patients with $Notch4^{low}$ expression were higher than those of patients with $Notch4^{high}$ expression (Fig. 7d, $P < 0.001$ by Wilcoxon test). Melanoma patients with both lymphatic metastasis and $Notch4^{high}$ expression had a worse prognosis than patients with lymphatic metastasis and $Notch4^{low}$ expression (Fig. 7d, $P < 0.001$ by Wilcoxon test). Therefore, our data show that $Notch4^{high}$ expression and metastasis are related to poor prognosis and that the combination of these two indices may serve as a prognostic indicator.

## Discussion

As is well known, melanoma is a highly lethal malignant tumor with a high rate of metastasis. Once metastatic, the outcomes for patients are poor.[32] Clarification of the mechanisms that underlie tumor metastasis is essential for the improvement in cancer survival of individuals with cancer. New targets and strategies are needed to improve the treatment of metastatic melanoma, especially for those patients who do not respond to conventional therapies. An in-depth understanding of melanoma biology and metastasis would greatly facilitate efforts in this area. Contrary to the use of other sphere formation models, the tumorosphere model is suitable for the study of CSC properties.[23] Sphere-forming cells, which were enriched in a serum-free culture system (tumorospheres) that were identified

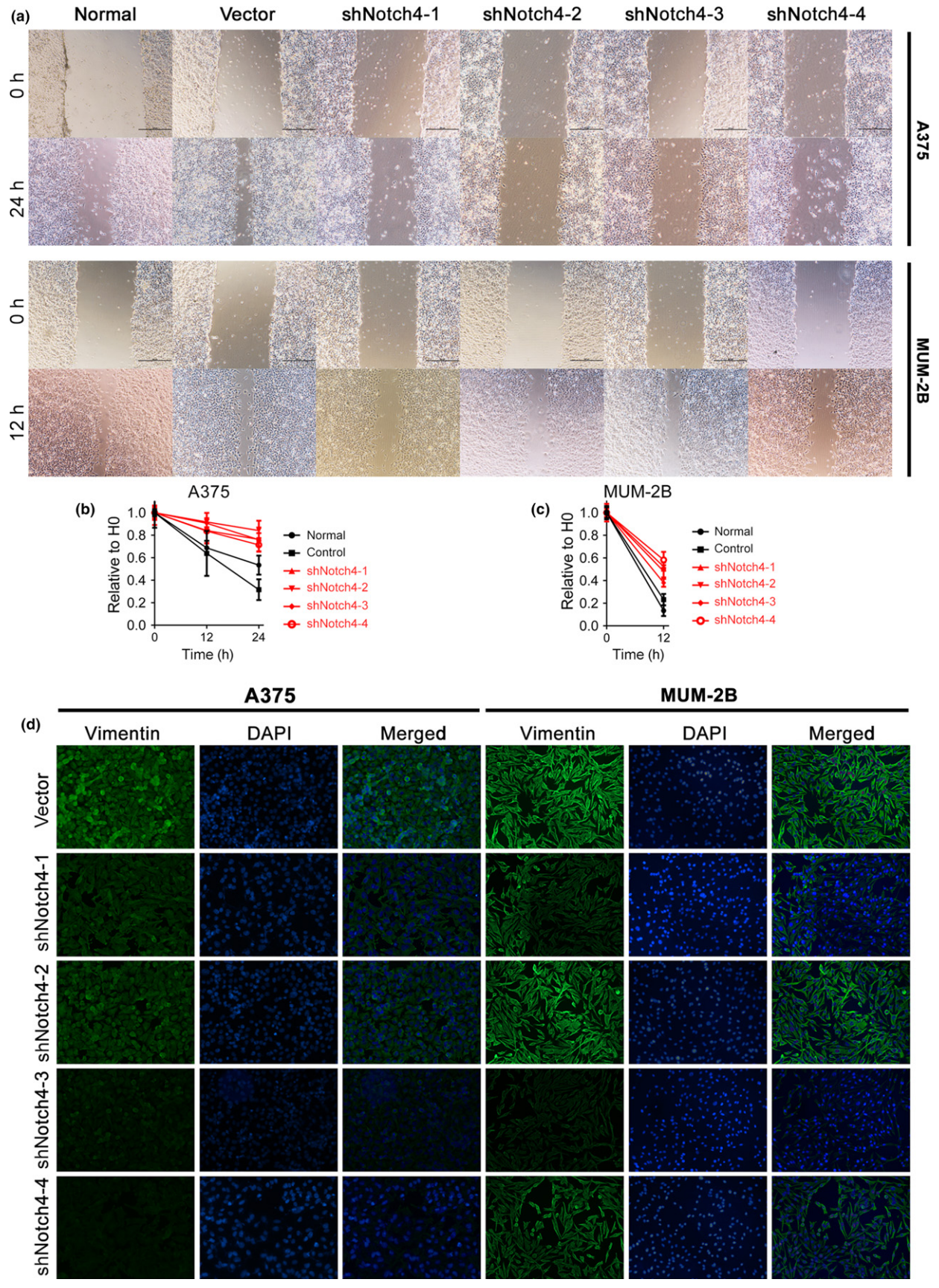


**Fig. 4.** Notch4 suppression inhibited the migration of melanoma cells and reduced vimentin expression. (a) Wound healing assay (magnification, ×40). (b,c) Quantitative analysis showed a significant difference at 24 h for A375 cells and showed a significant difference at 12 h for MUM-2B cells. (d) Knockdown of Notch4 decreased the protein expression of vimentin (magnification, ×200).

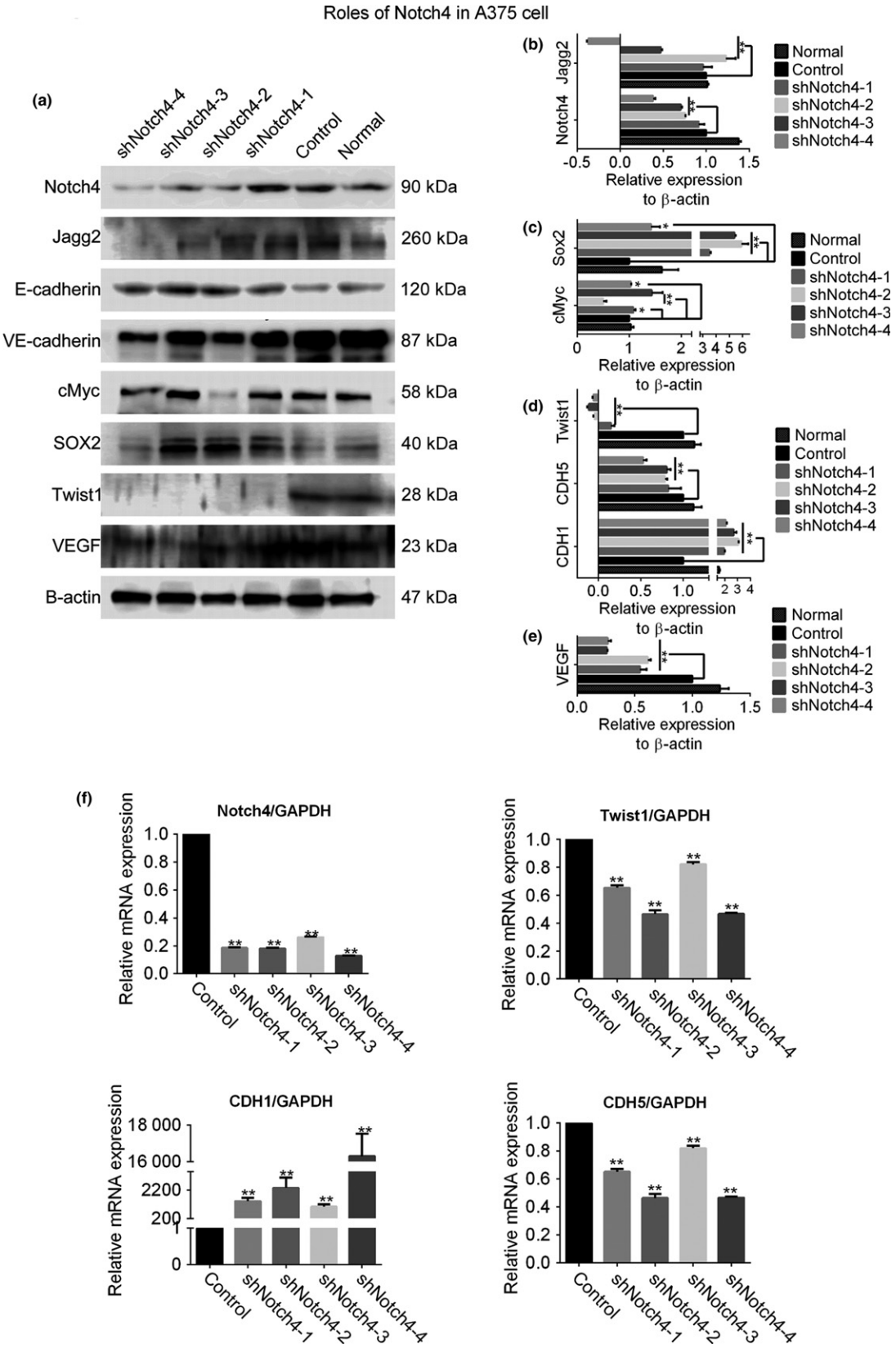


**Fig. 5.** Roles of Notch4 suppression in A375 melanoma cells. (a) Western blotting results. (b) Grey analysis revealed significantly decreased expression of Notch4 protein in A375 cells transfected with the shNotch4-2, -3, and -4 clones. (c) Sox2 expression was increased by shNotch4-2, -3, and -4. cMyc expression was increased by shNotch4-1, -3, and -4 clones and inhibited by the shNotch4-2 clone. (d) Notch4 suppression decreased Twist1 and VE-cadherin (CDH5) expression and increased E-cadherin expression. (e) Expression of the angiogenesis-related protein vascular endothelial growth factor (VEGF) was decreased when Notch4 expression was suppressed. (f) Quantitative real-time PCR results showed that *Notch4* silencing led to the upregulation of E-cadherin (*CDH1*) gene expression and a decrease in *Twist1* and VE-cadherin (*CDH5*) expression. $*P < 0.05$, $**P < 0.001$.

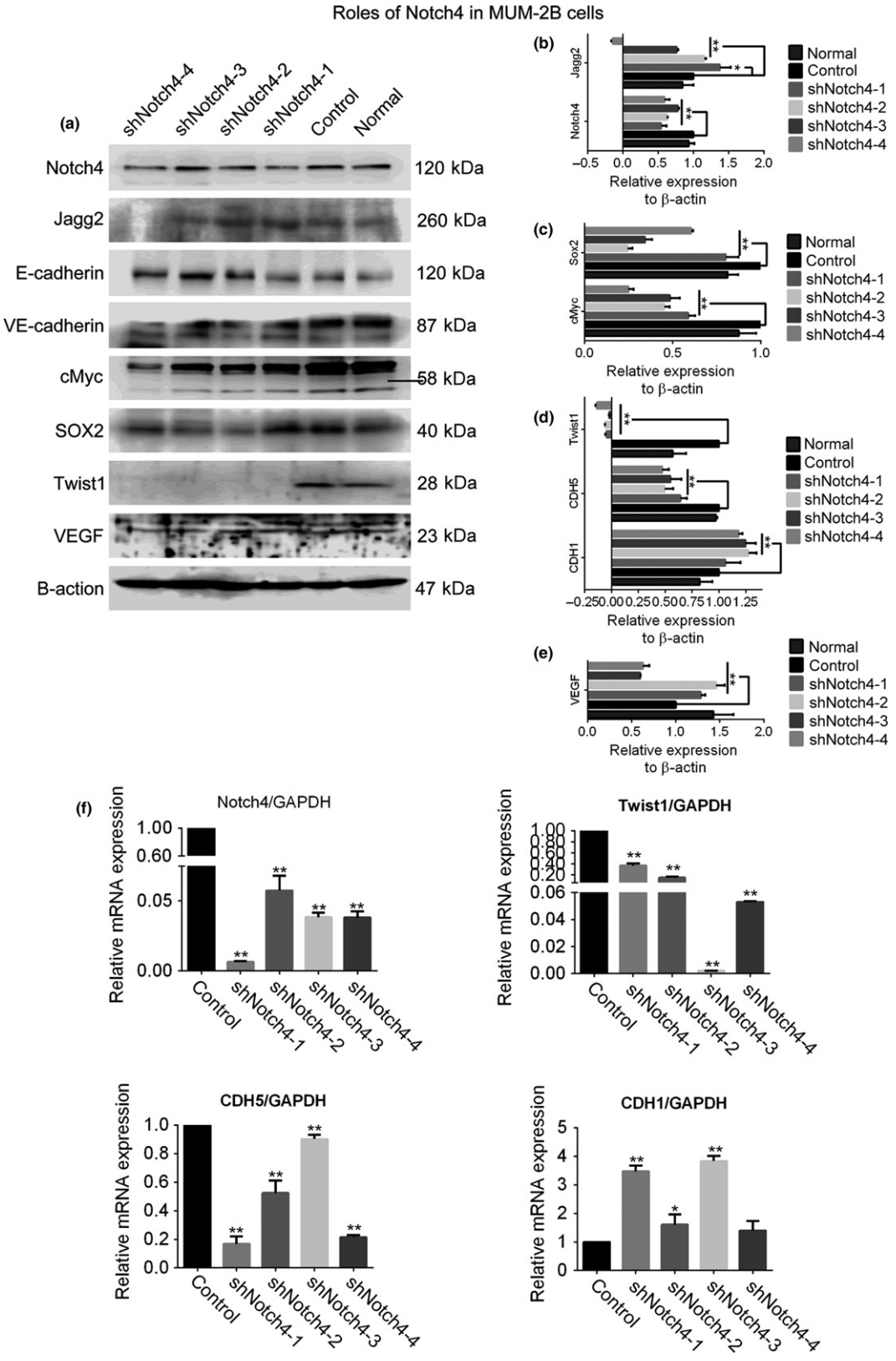


**Fig. 6.** Roles of Notch4 suppression in MUM-2B melanoma cells. (a) Western blotting results. (b) Grey analysis revealed a significantly decreased expression of Notch4 protein in MUM-2B cells transfected with the shNotch4-1, -2, -3, and -4 clones. (c) Sox2 expression was decreased by shNotch4-2, -3, and -4; Sox2 expression was increased by the shNotch4-1 clone. cMyc expression was inhibited by the shNotch4-1, -2, -3, and -4 clones. (d) Notch4 suppression decreased Twist1 and VE-cadherin (CDH5) expression and increased E-cadherin expression. (f) Expression of the angiogenesis-related protein vascular endothelial growth factor (VEGF) was decreased by shNotch4-3 and -4; in contrast, t was increased by the shNotch4-1 and -2 clones. (f) Quantitative real-time PCR results showed that *Notch4* silencing led to the upregulation of E-cadherin (*CDH1*) gene expression but led to a decrease in *Twist1* and VE-cadherin (*CDH5*) expression. $*P < 0.05$, $**P < 0.001$.

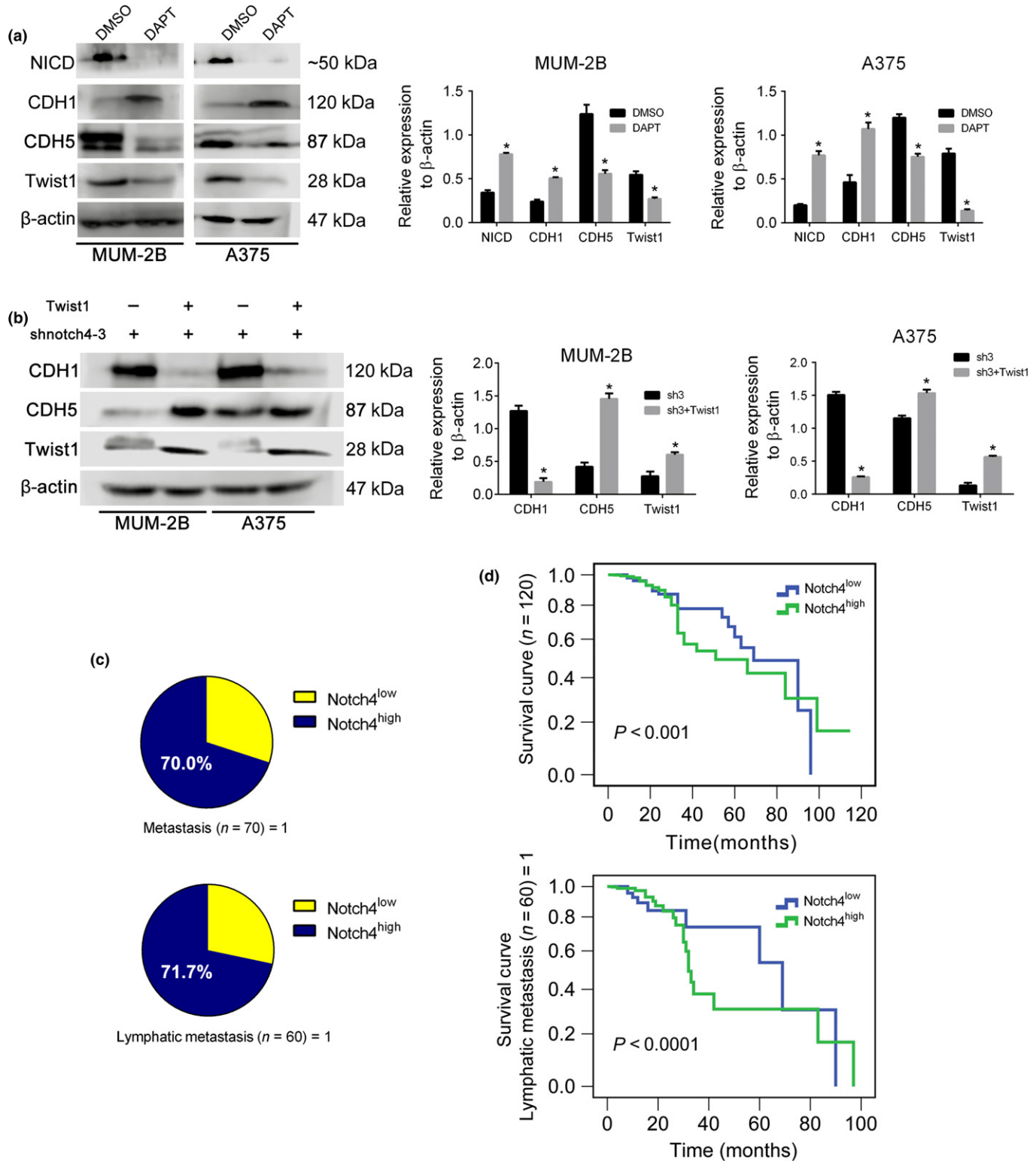


**Fig. 7.** *Notch4* silencing reduced epithelial–mesenchymal transition in melanoma cells through the Twist1/E-cadherin/VE-cadherin pathway, and high expression of Notch4 was found to be related to metastasis of melanoma and indicated a poor prognosis. (a) The γ-secretase inhibitor DAPT inhibited Twist1 and VE-cadherin (CDH5) expression and increased E-cadherin (CDH1) expression. (b) Notch4 suppression in cells increased VE-cadherin (CDH5) expression and decreased E-cadherin (CDH1) expression after the re-overexpression of Twist1 by transfection of cells with Twist1 expression clone. $*P < 0.05$. (c) 70% of patients with metastasis had tumors with high levels of Notch4 protein, and this was especially evident in patients with lymphatic metastasis. (d) The life table method indicated that high Notch4 expression was significantly related to poor prognosis. Patients with lymphatic metastasis and high expression of Notch4 had a worse prognosis. $P < 0.001$, for all.

**Table 1. Correlation of Notch4 expression with clinicopathological parameters of patients with melanoma**

| Variant | Notch4 expression | | $\chi^2$-test | *P*-value |
|---|---|---|---|---|
| | Low ($n$ = 48) | High ($n$ = 72) | | |
| Sex | | | | |
| Male | 36 | 45 | 2.051 | 0.169 |
| Female | 12 | 27 | | |
| Age, years | | | | |
| ≥55 | 35 | 39 | 0.047 | 0.055 |
| <55 | 13 | 33 | | |
| Tumor size, cm | | | | |
| ≥7.8 | 22 | 30 | 0.204 | 0.709 |
| <7.8 | 26 | 42 | | |
| AJCC staging | | | | |
| Stage I | 17 | 7 | 11.884 | 0.001* |
| Stage II + III + IV | 31 | 65 | | |
| Breslow's depth, mm | | | | |
| ≤1.5 | 16 | 28 | 0.947 | 0.623 |
| >1.5 | 32 | 44 | | |
| Pigments | | | | |
| Yes | 28 | 33 | 2.117 | 0.170 |
| No | 20 | 39 | | |
| Lymphatic metastasis | | | | |
| Yes | 16 | 43 | 6.806 | 0.015* |
| No | 32 | 29 | | |
| Distant metastasis | | | | |
| Yes | 14 | 28 | 1.197 | 0.331 |
| No | 34 | 44 | | |
| Lymphatic and/or distant metastasis | | | | |
| Yes | 21 | 49 | 7.000 | 0.014* |
| No | 27 | 23 | | |

*$P$ < 0.05. AJCC, American Joint Committee on Cancer.

as CSCs, possess the capacity for tumor invasion and metastasis, but are also resistant to conventional treatments.[20,33–36]

In this study, we used tumorospheres and a gene expression microarray to investigate the gene expression profile of MCSLCs. The gene expression microarray showed that MCSLCs expressed high levels of CSC markers, including SOX4, Wnt10a, and NGFR. Thus, we believe that the SFM system is appropriate for the isolation and enrichment of melanoma stem-like cells. Moreover, MCSLCs expressed high levels of the drug resistance gene *ABCA8*[37] as well as Notch signaling pathway molecules, including Notch3, Notch4, Dtx4, JAG2, and Pofut. The notch signaling pathway is a highly conserved signaling cascade that plays an essential role in the regulation of normal stem cell homeostasis and differentiation.[38–40] In oncogenesis, the dysregulation of the Notch and cancer stem cell pathways confers on many human tumors the ability to maintain a stem cell-like phenotype.[35,41–43] In our study, the detection of Notch4 expression by the immunofluorescence staining of sphere-forming cells also revealed that MCSLCs expressed high levels of Notch4.

Recently, aberrant Notch signaling observed in cancer stem cells and in metastatic tumors has attracted increasing attention, especially in melanoma, which is a particularly malignant tumor with high rates of Notch-related metastasis.[44–46] However, the expression of Notch in melanoma is not uniform. The loss of the cell adhesion molecule E-cadherin and the increased expression of the cell adhesion molecule VE-cadherin are correlated with EMT and with the invasion and metastasis of melanoma. Multiple groups have reported that amplified Notch signaling contributes to melanoma growth *in vitro* and *in vivo* and promotes a more aggressive phenotype, at least in part through the inhibition of E-cadherin expression.[47,48] However, other researchers have found that the high expression of Notch4 increases E-cadherin expression and suppresses malignant behavior of melanoma.[49] The authors reported that Notch4 induces suppression of Snail2 and Twist1 by downstream targets Hey1 and Hey2 and is mediated in a non-canonical fashion in melanoma cell lines WM9 and WM164. Mary Hendrix and his colleagues have reported that Notch4 promoted Nodal expression in metastatic melanoma cell lines C8161, MV3, and SK-MEL-28.[50] Nodal is a transforming growth factor-β superfamily member that promotes EMT.[51,52] It will be important for subsequent studies to extend findings in other cell lines and learn the relationships between Notch4 and EMT.

In this present study, we used melanoma cell lines B16F10, A375 and MUM-2B. Our results showed that Notch4$^{high}$ B16F10 cells expressed a lower level of E-cadherin and a higher level of VE-cadherin protein compared with Notch4$^{low}$ B16F10 cells. In the human melanoma A375 and MUM-2B cell lines, RT-PCR and Western blot analysis revealed that Notch4 silencing resulted in increased expression of E-cadherin and a loss of expression of VE-cadherin. Biologically, Notch4 silencing inhibited the migration and invasion of melanoma cells. Across our cohort, nearly 50% of melanomas showed high Notch4 protein expression. Moreover, high Notch4 expression is associated with metastasis and poor prognosis. We infer that Notch4 facilitates EMT and increases the invasive and metastatic behavior of melanoma.

The γ-secretase inhibitor DAPT inhibits the Notch signaling pathway through the inhibition of the release of intracellular domain.[53] Our results showed that both Notch4 silencing and DAPT application resulted in the loss of Twist1 expression. However, the overexpression of Twist1 by transfection of A375–shNotch4-3 and MUM-2B–shNotch4-3 cells with a Twist1 overexpression plasmid led to a decrease in E-cadherin expression and an increase in VE-cadherin expression. We conclude that Notch4 overexpression accelerates invasion and migration of melanoma through the regulation of Twist1 expression. Additionally, this work indicated that γ-secretase inhibitors may be used as a therapeutic strategy to inhibit the metastasis of melanoma.

The Notch signaling pathway plays an essential role in the regulation of angiogenesis during development and in adult life. Increasing evidence has revealed that the dysregulation of the Notch pathway promotes angiogenesis in tumors. Our results also indicated that high expression of Notch4 in A375 and MUM-2B cells can promote the formation of VM tubes. Additionally, Notch4 silencing decreased Matrigel-based tube formation. We infer that Notch4 expression may be related to VM formation in melanoma.[54] Tumor growth and metastasis depend on angiogenesis and lymphangiogenesis.[55] Angiogenesis inhibitors now constitute a clinical anticancer strategy.[56,57] Vascular endothelial growth factor is considered a key mediator of angiogenesis and a promising therapeutic target in cancer.[58–61] Our results showed that *Notch4* silencing downregulated the expression of VEGF. We suggest Notch4 may promote tumor angiogenesis by regulating VEGF expression.

In conclusion, MCSLCs were isolated and expanded using an SFM culture system. The enriched cancer stem-like cells showed high Notch4 expression. Moreover, Notch4 overexpression promotes the metastasis of melanoma through the

regulation of Twist1 expression, which indicates a poor prognosis. Our study suggests that Notch4 may be a valid target in melanoma treatment and thus requires further investigation.

## Acknowledgments

This study was supported by grants from the Key Project of the National Natural Science Foundation of China (Grant No. 81230050 to B.S.) and the National Natural Science Foundation of China (Grant No. 81572872 to X.Z.).

## Disclosure Statement

The authors have no conflict of interest.

## References

1 Bexell D, Gunnarsson S, Siesjo P, Bengzon J, Darabi A. CD133+ and nestin+ tumor-initiating cells dominate in N29 and N32 experimental gliomas. *Int J Cancer* 2009; **125**: 15–22.
2 Burgos-Ojeda D, Wu R, McLean K *et al.* CD24+ ovarian cancer cells are enriched for cancer-initiating cells and dependent on JAK2 signaling for growth and metastasis. *Mol Cancer Ther* 2015; **14**: 1717–27.
3 Chandrasekaran S, Delouise LA. Enriching and characterizing cancer stem cell sub-populations in the WM115 melanoma cell line. *Biomaterials* 2011; **32**: 9316–27.
4 Chiou SH, Wang ML, Chou YT *et al.* Coexpression of Oct4 and Nanog enhances malignancy in lung adenocarcinoma by inducing cancer stem cell-like properties and epithelial-mesenchymal transdifferentiation. *Cancer Res* 2010; **70**: 10433–44.
5 Dang H, Steinway SN, Ding W, Rountree CB. Induction of tumor initiation is dependent on CD44s in c-Met(+) hepatocellular carcinoma. *BMC Cancer* 2015; **15**: 161.
6 Adhikari AS, Agarwal N, Iwakuma T. Metastatic potential of tumor-initiating cells in solid tumors. *Front Biosci (Landmark Ed)* 2011; **16**: 1927–38.
7 Bleau AM, Zandueta C, Redrado M *et al.* Sphere-derived tumor cells exhibit impaired metastasis by a host-mediated quiescent phenotype. *Oncotarget* 2015; **6**: 27288–303.
8 Bozorgi A, Khazaei M, Khazaei MR. New findings on breast cancer stem cells: a review. *J Breast Cancer* 2015; **18**: 303–12.
9 Ooka H, Kanda S, Okazaki H *et al.* Characterization of side population (SP) cells in murine cochlear nucleus. *Acta Otolaryngol* 2012; **132**: 693–701.
10 Xie ZY, Lv K, Xiong Y, Guo WH. ABCG2-meditated multidrug resistance and tumor-initiating capacity of side population cells from colon cancer. *Oncol Res Treat* 2014; **37**: 666–8, 70-2.
11 Boiko AD, Razorenova OV, van de Rijn M *et al.* Human melanoma-initiating cells express neural crest nerve growth factor receptor CD271. *Nature* 2010; **466**: 133–7.
12 Czyz M, Koprowska K, Sztiller-Sikorska M. Parthenolide reduces the frequency of ABCB5-positive cells and clonogenic capacity of melanoma cells from anchorage independent melanospheres. *Cancer Biol Ther* 2013; **14**: 135–45.
13 Kinugasa Y, Matsui T, Takakura N. CD44 expressed on cancer-associated fibroblasts is a functional molecule supporting the stemness and drug resistance of malignant cancer cells in the tumor microenvironment. *Stem Cells* 2014; **32**: 145–56.
14 Lai CY, Schwartz BE, Hsu MY. CD133+ melanoma subpopulations contribute to perivascular niche morphogenesis and tumorigenicity through vasculogenic mimicry. *Cancer Res* 2012; **72**: 5111–8.
15 Weiswald LB, Bellet D, Dangles-Marie V. Spherical cancer models in tumor biology. *Neoplasia* 2015; **17**: 1–15.
16 Techawattanawisal W, Nakahama K, Komaki M, Abe M, Takagi Y, Morita I. Isolation of multipotent stem cells from adult rat periodontal ligament by neurosphere-forming culture system. *Biochem Biophys Res Commun* 2007; **357**: 917–23.
17 Chen X, Hu C, Zhang W *et al.* Metformin inhibits the proliferation, metastasis, and cancer stem-like sphere formation in osteosarcoma MG63 cells in vitro. *Tumour Biol* 2015; **36**: 9873–83.
18 Chen Z, Che Q, He X *et al.* Stem cell protein Piwil1 endowed endometrial cancer cells with stem-like properties via inducing epithelial-mesenchymal transition. *BMC Cancer* 2015; **15**: 811.
19 Ramgolam K, Lauriol J, Lalou C *et al.* Melanoma spheroids grown under neural crest cell conditions are highly plastic migratory/invasive tumor cells endowed with immunomodulator function. *PLoS ONE* 2011; **6**: e18784.
20 Cao L, Zhou Y, Zhai B *et al.* Sphere-forming cell subpopulations with cancer stem cell properties in human hepatoma cell lines. *BMC Gastroenterol* 2011; **11**: 71.
21 Hiraga T, Ito S, Nakamura H. Cancer stem-like cell marker CD44 promotes bone metastases by enhancing tumorigenicity, cell motility, and hyaluronan production. *Cancer Res* 2013; **73**: 4112–22.
22 Tham M, Khoo K, Yeo KP *et al.* Macrophage depletion reduces postsurgical tumor recurrence and metastatic growth in a spontaneous murine model of melanoma. *Oncotarget* 2015; **6**: 22857–68.
23 Yuhas JM, Li AP, Martinez AO, Ladman AJ. A simplified method for production and growth of multicellular tumor spheroids. *Cancer Res* 1977; **37**: 3639–43.
24 Francescone RA 3rd, Faibish M, Shao R. A Matrigel-based tube formation assay to assess the vasculogenic activity of tumor cells. *J Vis Exp* 2011; **55**: 3040.
25 Livak KJ, Schmittgen TD. Analysis of relative gene expression data using real-time quantitative PCR and the 2(T)(-Delta Delta C) method. *Methods* 2001; **25**: 402–8.
26 Zhao XL, Sun BC, Li YL *et al.* Dual effects of collagenase-3 on melanoma: metastasis promotion and disruption of vasculogenic mimicry. *Oncotarget* 2015; **6**: 8890–9.
27 Murphy GF, Wilson BJ, Girouard SD, Frank NY, Frank MH. Stem cells and targeted approaches to melanoma cure. *Mol Aspects Med* 2014; **39**: 33–49.
28 Hendrix MJ, Seftor EA, Meltzer PS *et al.* Expression and functional significance of VE-cadherin in aggressive human melanoma cells: role in vasculogenic mimicry. *Proc Natl Acad Sci USA* 2001; **98**: 8018–23.
29 Kuphal S, Palm HG, Poser I, Bosserhoff AK. Snail-regulated genes in malignant melanoma. *Melanoma Res* 2005; **15**: 305–13.
30 Noseda M, McLean G, Niessen K *et al.* Notch activation results in phenotypic and functional changes consistent with endothelial-to-mesenchymal transformation. *Circ Res* 2004; **94**: 910–7.
31 Sun T, Zhao N, Zhao XL *et al.* Expression and functional significance of Twist1 in hepatocellular carcinoma: its role in vasculogenic mimicry. *Hepatology* 2010; **51**: 545–56.
32 Kotlan B, Liszkay G, Blank M *et al.* The novel panel assay to define tumor-associated antigen-binding antibodies in patients with metastatic melanomas may have diagnostic value. *Immunol Res* 2015; **61**: 11–23.
33 Shi X, Gipp J, Bushman W. Anchorage-independent culture maintains prostate stem cells. *Dev Biol* 2007; **312**: 396–406.
34 Fujii H, Honoki K, Tsujiuchi T, Kido A, Yoshitani K, Takakura Y. Sphere-forming stem-like cell populations with drug resistance in human sarcoma cell lines. *Int J Oncol* 2009; **34**: 1381–6.
35 Grudzien P, Lo S, Albain KS *et al.* Inhibition of Notch signaling reduces the stem-like population of breast cancer cells and prevents mammosphere formation. *Anticancer Res* 2010; **30**: 3853–67.
36 Cioce M, Gherardi S, Viglietto G *et al.* Mammosphere-forming cells from breast cancer cell lines as a tool for the identification of CSC-like- and early progenitor-targeting drugs. *Cell Cycle* 2010; **9**: 2878–87.
37 Tsuruoka S, Ishibashi K, Yamamoto H *et al.* Functional analysis of ABCA8, a new drug transporter. *Biochem Biophys Res Commun* 2002; **298**: 41–5.
38 Geisler F, Strazzabosco M. Emerging roles of Notch signaling in liver disease. *Hepatology* 2015; **61**: 382–92.
39 Storck S, Delbos F, Stadler N *et al.* Normal immune system development in mice lacking the Deltex-1 RING finger domain. *Mol Cell Biol* 2005; **25**: 1437–45.
40 Dontu G, Jackson KW, McNicholas E, Kawamura MJ, Abdallah WM, Wicha MS. Role of Notch signaling in cell-fate determination of human mammary stem/progenitor cells. *Breast Cancer Res* 2004; **6**: R605–15.
41 Yao K, Rizzo P, Rajan P *et al.* Notch-1 and notch-4 receptors as prognostic markers in breast cancer. *Int J Surg Pathol* 2011; **19**: 607–13.
42 Hassan KA, Wang L, Korkaya H *et al.* Notch pathway activity identifies cells with cancer stem cell-like properties and correlates with worse survival in lung adenocarcinoma. *Clin Cancer Res* 2013; **19**: 1972–80.
43 Arasada RR, Amann JM, Rahman MA, Huppert SS, Carbone DP. EGFR blockade enriches for lung cancer stem-like cells through Notch3-dependent signaling. *Cancer Res* 2014; **74**: 5572–84.
44 Balint K, Xiao M, Pinnix CC *et al.* Activation of Notch1 signaling is required for beta-catenin-mediated human primary melanoma progression. *J Clin Investig* 2005; **115**: 3166–76.
45 Ding LC, She L, Zheng DL *et al.* Notch-4 contributes to the metastasis of salivary adenoid cystic carcinoma. *Oncol Rep* 2010; **24**: 363–8.

46 Asnaghi L, Ebrahimi KB, Schreck KC *et al.* Notch signaling promotes growth and invasion in uveal melanoma. *Clin Cancer Res* 2012; **18**: 654–65.
47 Leong KG, Niessen K, Kulic I *et al.* Jagged1-mediated Notch activation induces epithelial-to-mesenchymal transition through Slug-induced repression of E-cadherin. *J Exp Med* 2007; **204**: 2935–48.
48 Capaccione KM, Hong X, Morgan KM *et al.* Sox9 mediates Notch1-induced mesenchymal features in lung adenocarcinoma. *Oncotarget* 2014; **5**: 3636–50.
49 Bonyadi Rad E, Hammerlindl H, Wels C *et al.* Notch4 signaling induces a mesenchymal-epithelial-like transition in melanoma cells to suppress malignant behaviors. *Cancer Res* 2016; **76**: 1690–7.
50 Hardy KM, Kirschmann DA, Seftor EA *et al.* Regulation of the embryonic morphogen Nodal by Notch4 facilitates manifestation of the aggressive melanoma phenotype. *Cancer Res* 2010; **70**: 10340–50.
51 Guo Q, Ning F, Fang R *et al.* Endogenous Nodal promotes melanoma undergoing epithelial-mesenchymal transition via Snail and Slug in vitro and in vivo. *Am J Cancer Res* 2015; **5**: 2098-+.
52 Zavadil J, Bottinger EP. TGF-beta and epithelial-to-mesenchymal transitions. *Oncogene* 2005; **24**: 5764–74.
53 Borghese L, Dolezalova D, Opitz T *et al.* Inhibition of notch signaling in human embryonic stem cell-derived neural stem cells delays G1/S phase transition and accelerates neuronal differentiation in vitro and in vivo. *Stem Cells* 2010; **28**: 955–64.
54 Iwamoto H, Zhang Y, Seki T *et al.* PlGF-induced VEGFR1-dependent vascular remodeling determines opposing antitumor effects and drug resistance to Dll4-Notch inhibitors. *Sci Adv* 2015; **1**: e1400244.
55 Ji H, Cao R, Yang Y *et al.* TNFR1 mediates TNF-α-induced tumour lymphangiogenesis and metastasis by modulating VEGF-C-VEGFR3 signalling. *Nat Commun* 2014; **5**: 4944.
56 Hedlund EM, Yang X, Zhang Y *et al.* Tumor cell-derived placental growth factor sensitizes antiangiogenic and antitumor effects of anti-VEGF drugs. *Proc Natl Acad Sci USA* 2013; **110**: 654–9.
57 Cao Y. Future options of anti-angiogenic cancer therapy. *Chin J Cancer* 2016; **35**: 21.
58 Yang X, Zhang Y, Yang Y *et al.* Vascular endothelial growth factor-dependent spatiotemporal dual roles of placental growth factor in modulation of angiogenesis and tumor growth. *Proc Natl Acad Sci USA* 2013; **110**: 13932–7.
59 Cao Y. VEGF-targeted cancer therapeutics[mdash]paradoxical effects in endocrine organs. *Nat Rev Endocrinol* 2014; **10**: 530–9.
60 Jensen LD, Nakamura M, Brautigam L *et al.* VEGF-B-Neuropilin-1 signaling is spatiotemporally indispensable for vascular and neuronal development in zebrafish. *Proc Natl Acad Sci USA* 2015; **112**: E5944–53.
61 Yang X, Zhang Y, Hosaka K *et al.* VEGF-B promotes cancer metastasis through a VEGF-A–independent mechanism and serves as a marker of poor prognosis for cancer patients. *Proc Natl Acad Sci USA* 2015; **112**: E2900–9.

## Supporting Information

Additional Supporting Information may be found online in the supporting information tab for this article:

**Fig. S1.** Morphological differences. First-generation and third-generation melanoma cancer stem-like cells that were obtained in a serum-free culture system (tumorospheres) and multicellular tumor spheroid cells are pictured. Hematoxylin–eosin staining of these two types of spheres is shown.

**Table S1** Details of antibodies used in this study.

**Table S2** Primer sequences of quantitative RT-PCR and shRNA target sequences of Notch4.

**Table S3** Clinicopathological parameters of 120 melanoma cases.

**Table S4** Life table method in 120 melanoma patients.